ChemComm

Accepted Manuscript

This is an *Accepted Manuscript*, which has been through the Royal Society of Chemistry peer review process and has been accepted for publication.

Accepted Manuscripts are published online shortly after acceptance, before technical editing, formatting and proof reading. Using this free service, authors can make their results available to the community, in citable form, before we publish the edited article. We will replace this *Accepted Manuscript* with the edited and formatted *Advance Article* as soon as it is available.

You can find more information about *Accepted Manuscripts* in the **Information for Authors**.

ChemComm

COMMUNICATION

Plasmon-induced spatial electron transfer between single Au nanorod and ALD-coated TiO₂: dependence on TiO₂ thickness

Zhaoke Zheng,[a] Takashi Tachikawa,[b] and Tetsuro Majima*[a]

We employed single-particle photoluminescence (PL) measurements to investigate the interfacial electron transfer between single Au nanorod (NR) and TiO₂ coated by ALD. Analyzing the energy relaxation path of plasmon-generated hot electrons as well the PL intensities allowed for the detection and study of the interfacial electron transfer process spatially.

The efficient conversion of solar energy to electric or chemical energy has become a common concern in the world. Up to date, titanium dioxide has been extensively studied because of its applications towards photocatalytic water splitting, solar cells and degradation of organic pollutants, and has been one of the most promising and popular oxide semiconductors.[1-4] However, the large band gap of TiO₂ has critically restrained its photo-driven applications. To date, various approaches have been proposed to make TiO₂ sensitive to the visible and even near-infrared light.[5-8] Among various light-trapping techniques, the use of metallic nanostructures that support surface plasmons is an efficient route for broadening and enhancing the light absorption of TiO₂ through electric field enhancement and hot electron injection.[9-12] For instance, Au nanoparticles (NPs) are combined with TiO₂ to enhance the photocatalytic hydrogen production, photo-degradation, and performance of various solar cells.[13-16] To investigate the plasmon-induced charge-transfer mechanisms between excited Au NPs and TiO₂, ultrafast pump-probe femtosecond transient absorption spectroscopy was employed,[14,17,18] and such an electron transfer process was reported to be less than 100 fs. Although the electron-transfer mechanisms have been intensively studied, most of them are focused on the dynamics. The spatial-related interfacial electron transfer mechanism was

rarely reported. Furthermore, in these studies, mainly Au nanospheres are adsorbed on or embedded in TiO₂. While Au nanorods (NRs), with broadly tunable aspect-ratio-dependent longitudinal SPR (LSPR), was integrated with TiO₂ only in a limited number of studies.[16,19]

To investigate the spatial electron transfer mechanism from single Au NR to TiO₂, homogeneous coating of TiO₂ on Au NRs with precisely controllable shell thickness is very essential, because the electron transfer is sensitive to the shell thickness even at sub-nanometer level. However, there is little report about the precise and controllable coating of semiconductor onto Au NRs. Among all the coating method, atomic layer deposition (ALD) appears to be one of the most promising techniques, which can provide a precise thickness control at the Angstrom or monolayer level.[20-22] Furthermore, high aspect ratio structures can also be precisely coated by ALD.

In this study, we employed single-particle photoluminescence (PL) spectroscopy to investigate the interfacial electron transfer between single Au NR and TiO₂ precisely coated by ALD. The spatial electron transfer was studied by varying the thickness of TiO₂ from 1 to 5 nm. It is observed that the interfacial electron transfer is closely related to the thickness and the band structure of the adjacent electron acceptor. Computational simulation using the finite difference time domain (FDTD) method was also performed to support our conclusions.

The inset in Fig. 1a shows a representative TEM image of single TiO₂-coated Au NR with thickness of 2 nm. An amorphous TiO₂ shell was homogeneously deposited on the surface of Au NR, and the thickness agrees well with the expected values (50 cycles, 2 nm). Because the sample that consists of mono-dispersed Au NRs and a thin TiO₂ layer (less than 5 nm) was colorless, it is difficult to measure the extinction spectra *via* experimental method. We thus carried out FDTD calculations on the single TiO₂-coated Au NRs. The FDTD simulation can provide a full range of SPR-related optical properties including extinction spectrum, local electric field enhancement, and so on. The extinction spectra at LSPR region

a. *The Institute of Scientific and Industrial Research (SANKEN), Osaka University, Mihogaoka 8-1, Ibaraki, Osaka 567-0047, Japan*
b. *Department of Chemistry, Graduate School of Science, Kobe University, 1-1 Rokkodai-cho, Nada-ku, Kobe 657-8501, Japan*

Fig. 1 (a) PL image of single Au NR dispersed on quartz cover glass. The inset shows representative TEM image of single TiO_2-coated Au NR with thickness of 2 nm. PL spectra of the single Au NR (b) and single TiO_2-coated Au NR with different shell thickness (c-f). Two randomly measured PL spectra of single NR are shown for each sample. The insets in panel b and c show the magnified image of the selected region.

were obtained by setting the incident light polarization direction parallel to the longitudinal direction of single Au NR. As shown in Fig. S2d and S3, the LSPR peak in the calculated extinction spectra exhibit a red shift as increasing the shell thickness from 1 to 5 nm. Such a shell-thickness-depended peak-shift is in agreement with those from both experimental measurements and calculations.[23]

To investigate the light-induced interfacial electron transfer between single Au NR and TiO_2, single-particle PL measurements were carried out with a 485 nm laser. Fig. 1a shows a typical single-particle PL image of Au NRs dispersed on quartz cover glass. Since we want to obtain the statistical PL evolution of Au NRs before and after TiO_2-coating with different thickness, the mono-dispersibility of NRs is an essential requirement. Fig. S4 show typical SEM images of mono-dispersed Au NRs on quartz cover glass substrate, which confirms the mono-dispersibility of our sample. The PL spectra of two representative single Au NRs, collected by switching the detection to a spectrometer equipped with an EMCCD camera, are shown in Fig. 1b. A strong PL peak at the LSPR region was observed for each sample. The PL at the transversal surface plasmon resonance (TSPR) region was not fully displayed, owing to that a long pass filter ($\lambda > 513$ nm) was installed to completely remove the excitation light. This also indicates that the peak position of the TSPR PL over pure Au NRs is below 513 nm.

The PL spectra of the single TiO_2-coated Au NR with different shell thickness were obtained in the same manner (Fig. 1c-f). For the Au NRs coated with TiO_2 with thickness of 1 nm (Fig. 1c), there is no obvious change for the intensity of LSPR PL compared with that of the naked Au NRs (Fig. 1b). However, there is a conspicuous red shift of the TSPR PL peak (as shown in the insets of Fig. 1b-c), and the TSPR maximum begins to be visually observed. Normally, only the LSPR PL
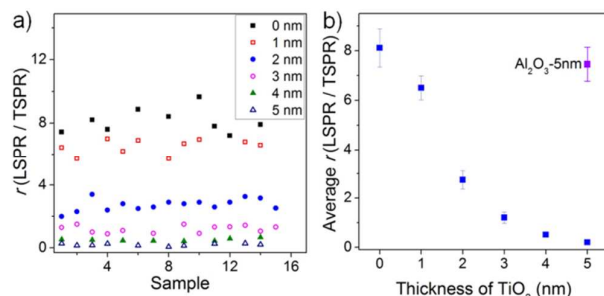
Fig. 2 (a) The ratio of LSPR PL intensity to TSPR PL intensity for tens of single TiO_2-coated Au NR with different shell thickness. (b) The average ratio of LSPR PL intensity to TSPR PL intensity for TiO_2-coated Au NRs and Al_2O_3-coated Au NRs with thickness of 5 nm.

peak position of Au NRs is sensitive to the aspect ratio while the TSPR PL maximum remains constant.[24,25] To investigate such a red shift of TSPR PL peak, the extinction spectra for TiO_2-coated Au NRs with various shell thicknesses were calculated by the FDTD simulation, while the refractive index of the ambient medium was taken to be 1, simulating the atmospherical conditions in single-particle PL experiment. As shown in Fig. S5, the TSPR maximum of TiO_2-coated Au NRs exhibit continuously red shift as increasing the thickness of TiO_2 shell from 1 to 5 nm, owing to the larger refractive index of TiO_2 compared with air. Therefore, the TSPR PL maximum moved to the longer wavelength correspondingly. On the other hand, such a red shift of TSPR maximum in Fig. 1c confirmed the successful coating of TiO_2. Further increasing the thickness of TiO_2, the PL intensities at the LSPR region dramatically decreased while the TSPR PL intensities remained unchanged. When the thickness of the TiO_2 shell increased to 5 nm, the PL at the LSPR region was almost totally quenched. Although the LSPR PL maximum is related to the aspect ratio of Au NRs, we found a general red-shift of peak position, which is consist with the extinction spectra calculations shown in Fig. S2d.

With the same method, we obtained tens of PL spectra of single TiO_2-coated Au NR with various shell thickness and six representative PL spectra are shown in Fig. S7-12 for each sample. We may notice that the absolute values of the PL intensities are different for various Au NRs even with the same coating thickness (Fig. S7-12), which is because the PL intensity is related to the volume of single NR and the chemical synthesized nanostructures have a morphological heterogeneity. Even though, the PL spectra can be analyzed statistically, since both the LSPR and TSPR PL intensities of Au NRs are related to their volume, and the quenching effect can be investigated by analyzing the ratio (r) of LSPR PL intensity to TSPR PL intensity. Considering that the TSPR PL intensity did not change after TiO_2 coating, such a ratio can represent the quenching efficiency of LSPR PL to a great extent.

By analyzing the PL spectra for 64 single Au NRs coated with different layers of TiO_2, we obtained the intensity ratios of LSPR PL to TSPR PL (Fig. 2a). To make the results more

ChemComm

COMMUNICATION

intuitive, the average ratio and the standard deviation were analyzed by descriptive statistics (Fig. 2b). As can be seen, for the naked Au NRs, the LSPR PL intensity was much higher than that of TSPR PL and the corresponding ratio was as high as 8. As increasing the thickness of TiO_2 shell, the LSPR PL intensity gradually decreased, indicating that the PL at the LSPR mode was quenched by the coated TiO_2 shell, and the quenching effect was enhanced as increasing the thickness of TiO_2. When the thickness of TiO_2 shell was over 3 nm, the PL intensity of at the LSPR mode was even lower than that at the TSPR mode (average $r < 1$), while the TSPR PL intensity remained unchanged since it is only relative to the volume of the Au NRs.[26] Notably, the PL at the LSPR mode was even totally quenched as the thickness of TiO_2 increased to 5 nm.

In our single-particle PL measurement, the interband transition of Au NRs was excited with 485 nm laser light and created electron-hole pairs, which can relax very efficiently through a fast interconversion with the TSPR mode and subsequently decays radiatively, leading to the short-wavelength PL peak.[27] Meanwhile, the hot electrons lose their energy nonradiatively and interconvert to the LSPR mode, which subsequently emits a photon, leading the LSPR PL (Fig. 3a). It has been reported that the luminescence from TSPR mode has a shorter lifetime (~5 fs) compared with that of LSPR mode (9~18 fs).[25] This means that the LSPR PL is more easily to be influenced by some other decay routes, while the TSPR PL is more related to its intrinsic features and invariant. In our case, when the Au NRs were coated with a layer of TiO_2, the hot electrons can also transfer from Au NRs to the TiO_2 shell, which competes with the LSPR emission and hence gives rise to the PL damping. The enhanced quenching effect with increasing the thickness of TiO_2 indicates a more efficient electron transfer from Au to TiO_2. The coating of TiO_2 will influence the extinction proprieties of Au NRs, and hence influence the PL intensity. However, the FDTD calculation shows that the extinction intensity only slightly decreased as increasing the TiO_2 thickness (Fig. S13), indicating that the obvious PL quenching was mainly due to the electron transfer process.

To further verify that the quenching phenomenon of TiO_2-coated Au NRs is resulting from the electron transfer behavior but not the coating effect, the single-particle PL of Al_2O_3-coated Au NRs with thickness of 5 nm were also measured (Fig. S14 and 2b). Similar to the TiO_2-coated Au NRs, the TSPR PL peak shifted to the longer wavelength and the TSPR maximum became to be visually observed, which was due to the larger refractive index of Al_2O_3 compared with air. Such a red shift also indicates that Au NRs were successfully coated by Al_2O_3. No quenching effect of LSPR PL was observed and the average ratio of Al_2O_3-coated Au NRs was even comparable to that of naked Au NRs, owing to that the conduction band position of Al_2O_3 is much higher than that of TiO_2, and hence the hot electrons of Au NRs excited at 485 nm do not have enough energy to move to the conduction band of Al_2O_3.

In the former studies about the electron transfer between Au and TiO_2, normally the size of TiO_2 is relatively large compared with that of Au NPs, and no size or spatial influence
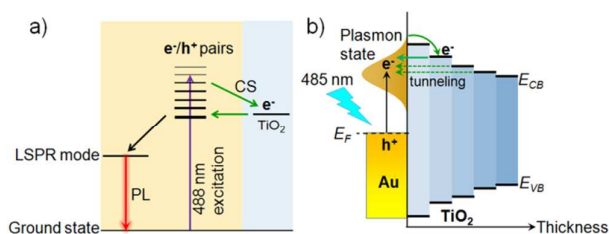
Fig. 3 Schematic diagram of the mechanism for radiative decay of surface plasmon (a) and interfacial electron transfer between single Au NR and TiO_2 (b). The solid purple line represents excitation with 485 nm continuous wave laser light. The charge separation state, CS, the Fermi energy, E_F, the valence (E_{VB}) and conduction band edges (E_{CB}) of the semiconductor.

was investigated at such a fine scale. When the thickness of TiO_2 was 5 nm, the nearly totally quenching of the LSPR PL demonstrates that the hot electrons transfer across the interface and are further trapped by TiO_2, since the hot electrons used for the LSPR emission are depleted. As decreasing the thickness of TiO_2, the PL at the LSPR mode still existed, especially for the thin layer with thickness of 1~2 nm. One of the reasons is due to the quantum size effects. A decrease in size raises the conduction band and lowers the valence band, leading to the widened bandgap. For TiO_2 nanoparticles, a bandgap shift of 0.15 eV was observed with size of 2.4 nm.[28] It has been predicted that the bandgap energy for TiO_2 dramatically increases from 2 nm to 1 nm.[29] Similar quantum size effects in crystallized and amorphous TiO_2 thin layers were also reported.[30,31] In our case, TiO_2 has higher conduction band as decreasing the layer thickness, thus the hot electrons were difficult to transfer to the E_{CB} of TiO_2. When the layer thickness was over 2 nm, an obvious quenching phenomenon occurred due to the lower E_{CB} of TiO_2 and hence an efficient electron transfer. Meanwhile, the electrons that transferred to the conduction band of TiO_2 can further move back to the Au NRs within such a short distance, similar to the tunneling effect.[32] Such energetic electrons can further decay and interconvert to the LSPR mode and emits. The back transfer effect is more apparent for the NRs with a thinner TiO_2 layer. That is why the LSPR PL intensity is still very high for the Au NRs coated by TiO_2 with a thickness as thin as 1 nm. The above results also show that TiO_2 shell with a thickness of 5 nm is enough for trapping the hot electrons transferred from Au NRs.

In conclusion, we investigated the interfacial electron transfer behavior between single Au NR and TiO_2 shell by comparing the single-particle PL spectroscopy. The thickness of TiO_2 shell can be precisely controlled from 1 to 5 nm with the ALD method. The result shows that the interfacial electron transfer is closely related to the thickness and the band structure of the adjacent electron acceptor. Since the PL at the LSPR mode is sensitive to the interfacial electron transfer process, it can be employed as an efficient detector for the electron transfer in other systems. The finding obtained here

will help us to further understand the spatial electron transfer mechanism between Au and semiconductor photocatalysts.

Notes and references

1 Y. Ohko, T. Tatsuma, T. Fujii, K. Naoi, C. Niwa, Y. Kubota and A. Fujishima, *Nat. Mater.*, 2003, **2**, 29-31.
2 X. Chen and S. S. Mao, *Chem. Rev.*, 2007, **107**, 2891-2959.
3 W. E. Kaden, T. Wu, W. A. Kunkel and S. L. Anderson, *Science*, 2009, **326**, 826-829.
4 J. Burschka, N. Pellet, S. J. Moon, R. Humphry-Baker, P. Gao, M. K. Nazeeruddin and M. Gratzel, *Nature*, 2013, **499**, 316-319.
5 X. Chen, L. Liu, P. Y. Yu and S. S. Mao, *Science*, 2011, **331**, 746-750.
6 Z. K. Zheng, B. B. Huang, X. D. Meng, J. P. Wang, S. Y. Wang, Z. Z. Lou, Z. Y. Wang, X. Y. Qin, X. Y. Zhang and Y. Dai, *Chem. Commun.*, 2013, **49**, 868-870.
7 H. Tada, T. Mitsui, T. Kiyonaga, T. Akita and K. Tanaka, *Nat. Mater.*, 2006, **5**, 782-786.
8 Z. K. Zheng, B. B. Huang, J. B. Lu, Z. Y. Wang, X. Y. Qin, X. Y. Zhang, Y. Dai and M. H. Whangbo, *Chem. Commun.*, 2012, **48**, 5733-5735.
9 S. Linic, P. Christopher and D. B. Ingram, *Nat. Mater.*, 2011, **10**, 911-921.
10 H. A. Atwater and A. Polman, *Nat. Mater.*, 2010, **9**, 205-213.
11 S. Mubeen, G. Hernandez-Sosa, D. Moses, J. Lee and M. Moskovits, *Nano Lett.*, 2011, **11**, 5548-5552.
12 T. Tachikawa, T. Yonezawa and T. Majima, *ACS Nano*, 2013, **7**, 263-275.
13 Z. K. Zheng, B. B. Huang, X. Y. Qin, X. Y. Zhang, Y. Dai and M. H. Whangbo, *J. Mater. Chem.*, 2011, **21**, 9079-9087.
14 Z. Bian, T. Tachikawa, P. Zhang, M. Fujitsuka and T. Majima, *J. Am. Chem. Soc.*, 2014, **136**, 458-465.
15 M. D. Brown, T. Suteewong, R. S. Kumar, V. D'Innocenzo, A. Petrozza, M. M. Lee, U. Wiesner and H. J. Snaith, *Nano Lett.*, 2011, **11**, 438-445.
16 C. H. Fang, H. L. Jia, S. Chang, Q. F. Ruan, P. Wang, T. Chen and J. F. Wang, *Energy Environ. Sci.*, 2014, **7**, 3431-3438.
17 Y. Tian and T. Tatsuma, *J. Am. Chem. Soc.*, 2005, **127**, 7632-7637.
18 L. C. Du, A. Furube, K. Yamamoto, K. Hara, R. Katoh and M. Tachiya, *J. Phys. Chem. C*, 2009, **113**, 6454-6462.
19 L. Liu, S. Ouyang and J. Ye, *Angew. Chem. Int. Ed.*, 2013, **52**, 6689-6693.
20 C. Marichy, M. Bechelany and N. Pinna, *Adv. Mater.*, 2012, **24**, 1017-1032.
21 S. M. George, *Chem. Rev.*, 2010, **110**, 111-131.
22 M. Heikkilä, E. Puukilainen, M. Ritala and M. Leskelä, *J. Photochem. Photobiol., A*, 2009, **204**, 200–208.
23 X. Shi, Y. Ji, S. Hou, W. Liu, H. Zhang, T. Wen, J. Yan, M. Song, Z. Hu and X. Wu, *Langmuir*, 2015, **31**, 1537-1546.
24 Z. K. Zheng, T. Tachikawa and T. Majima, *J. Am. Chem. Soc.*, 2014, **136**, 6870-6873.
25 F. Wackenhut, A. V. Failla and A. J. Meixner, *J. Phys. Chem. C*, 2013, **117**, 17870-17877.
26 Z. K. Zheng, T. Tachikawa and T. Majima, *J. Am. Chem. Soc.*, 2015, **137**, 948-957.
27 A. Tcherniak, S. Dominguez-Medina, W.-S. Chang, P. Swanglap, L. S. Slaughter, C. F. Landes and S. Link, *J. Phys. Chem. C*, 2011, **115**, 15938-15949.
28 C. Kormann, D. W. Bahnemann and M. R. Hoffmann, *J. Phys. Chem.*, 1988, **92**, 5196-5201.
29 N. Satoh, T. Nakashima, K. Kamikura and K. Yamamoto, *Nat. Nanotechnol*, 2008, **3**, 106-111.
30 Y. H. Chang, C. M. Liu, H. E. Cheng and C. Chen, *ACS Appl Mater Interfaces*, 2013, **5**, 3549-3555.
31 D. M. King, X. H. Du, A. S. Cavanagh and A. Weimer, *Nanotechnology*, 2008, **19**.
32. C. Prasittichai, J. R. Avila, O. K. Farha and J. T. Hupp, *J. Am. Chem. Soc.*, 2013, **135**, 16328-16331.

ChemComm Accepted Manuscript